

Article

Visualizing Individual Tree Differences in Tree-Ring Studies

Mario Trouillier ^{1,*}, Marieke van der Maaten-Theunissen ², Jill E. Harvey ¹ , David Würth ³,
Martin Schnittler ³ and Martin Wilmking ¹ 

¹ Landscape Ecology and Ecosystem Dynamics Working Group, Institute of Botany and Landscape Ecology, University Greifswald, D-17487 Greifswald, Germany; harveyj@uni-greifswald.de (J.E.H.); wilmking@uni-greifswald.de (M.W.)

² Forest Growth and Woody Biomass Production, TU Dresden, D-01737 Tharandt, Germany; marieke.theunissen@tu-dresden.de

³ General and Special Botany Working Group, Institute of Botany and Landscape Ecology, University Greifswald, D-17487 Greifswald, Germany; david.wuerth@uni-greifswald.de (D.W.); mschnittl@uni-greifswald.de (M.S.)

* Correspondence: mario.trouillier@uni-greifswald.de; Tel.: +49-038-34420-4135

Received: 29 March 2018; Accepted: 16 April 2018; Published: 19 April 2018



Abstract: Averaging tree-ring measurements from multiple individuals is one of the most common procedures in dendrochronology. It serves to filter out noise from individual differences between trees, such as competition, height, and micro-site effects, which ideally results in a site chronology sensitive to regional scale factors such as climate. However, the climate sensitivity of individual trees can be modulated by factors like competition, height, and nitrogen deposition, calling attention to whether average chronologies adequately assess climatic growth-control. In this study, we demonstrate four simple but effective methods to visually assess differences between individual trees. Using individual tree climate-correlations we: (1) employed jitter plots with superimposed metadata to assess potential causes for these differences; (2) plotted the frequency distributions of climate correlations over time as heat maps; (3) mapped the spatial distribution of climate sensitivity over time to assess spatio-temporal dynamics; and (4) used t-distributed Stochastic Neighborhood Embedding (t-SNE) to assess which trees were generally more similar in terms of their tree-ring pattern and their correlation with climate variables. This suite of exploratory methods can indicate if individuals in tree-ring datasets respond differently to climate variability, and therefore, should not solely be explored with climate correlations of the mean population chronology.

Keywords: climate–growth relationships; averaging; individual based; dendrochronology

1. Introduction

1.1. Background

One of the most fundamental methods used in tree-ring studies involves averaging yearly tree-ring measurements from multiple individuals. The resulting chronology is often referred to as the site, population, or master chronology [1,2]. As is the case in many other disciplines, averaging replicated measurements serves to reduce individual noise and avoids pseudoreplications in statistical analyses [1–5]. Tree-ring variables, including width, density, and/or isotope concentration, are affected by various biotic and abiotic parameters, and when combined are often referred to as the ‘principle of aggregated tree growth’ [2,3,6,7]. Therefore, the chronology of each individual tree is the unique product of multiple signals. Differences between trees can originate from competition, microsite differences, age, size, physical damage, or asynchronous masting [2,3,8]. Therefore, it appears desirable

to average measurements from multiple trees to reduce this within-site variance and filter out the population-level signal(s). Particularly on the regional and landscape scale, or along large-scale environmental gradients like latitude, such mean chronologies are of great value to assess drivers of tree growth [9–11]. In such studies, it seems reasonable to assume that climate parameters affect all trees in a population similarly, and that the population signal largely contains climate signals.

It is desirable to quantify the effect of all parameters on tree growth; however, this is not yet possible. Explanatory variables of soil, micro-site conditions, root systems, or competition, available in a sufficient spatial and temporal resolution, are often not documented, nor are all the resultant physiological processes associated with tree-ring formation understood. Additionally, statistics require large sample sizes to detect small effects, which is critical if tree growth is the sum of many small effects [3,7]. Lastly, environmental variables often interact and can have ambiguous effects on different physiological processes, for example, higher temperatures might increase the speed of chemical processes in radial tree growth, but conversely, can cause drought stress by increasing evapotranspiration. Even though tree growth appears highly complex, few research fields outside tree-ring science can access samples from specimens that yield century-spanning records of individualistic reactions to the environment. Such valuable datasets should be evaluated as thoroughly as possible; therefore, in this manuscript, we outline four methods to visualize and explore individual tree differences.

1.2. Sampling and Data Processing

Various methods and principles have been established to build and evaluate population chronologies. Each study begins with selection of the sampling design, which inherently depends on the research question. It has been both criticized and defended that trees and sites are frequently selected systematically and non-randomly [2,12]. Generally, trees with high ring-width variability indicate that the growth-limiting factor varies between years, for example, climate. Such trees are preferred over complacent trees [3], which might rather be limited by a factor that does not vary greatly interannually, for example, light. Less sensitive trees might require a higher sample size per site than just 20–30 individuals [2]. It is common practice in dendrochronology to sample only specific sites or individuals. For example, treeline sites are often preferred because climate conditions at these sites are assumed to impose greater limitations on growth than competition [13]. On the individual level, tall, old, and dominant trees are often preferentially sampled. Generally, these sampling procedures, just as the averaging of multiple trees, serve to filter out individual ‘noise’. Similarly, individuals that do not correlate well with the rest of the population are often excluded when creating a population chronology with the intention to reduce ‘noise’. Next, the resulting population chronology is often described with various statistical measures to quantify the signal–noise ratio (SNR) [14], the mean sensitivity (MSX) [15], the shared growth variance of trees—subsample signal strength (SSS), or the commonly used expressed population signal (EPS), with its debated threshold of 0.85 [14,16,17]. Apart from reporting these statistical measures, these values cannot directly enhance the interpretation of analyses like climate correlations. This is because these measures relate to the cumulative effect of all biotic and abiotic variables on tree growth, not just single variables. Additionally, the underlying data distributions of these statistical measures or causes of high and low values are rarely explored.

Chronology averaging also makes the assumption that frequency distributions of social status, age classes, and tree density per area do not significantly change over time. The interactions of individual trees are also lost through averaging, when in theory, emergent properties develop from interacting elements within a system that cannot be explained by the sum or mean of the elements. For example, in tree-ring studies, individual trees interact via competition or facilitation, which can lead to subsequent changes in forest structure (e.g., tree density, crown shape, above/below ground biomass allocation) [18–21], and further confound the explanation of tree-growth variability. Single trees are rarely the main focus of dendrochronological or dendroclimatological studies, with the possible

exception of very old individuals or individuals, such as the “Loneliest Tree in the World” [22,23], however, increasingly, studies do analyze individual tree differences [21,24–31].

Of course, mean population chronologies remain a useful tool to explore how a population reacts on average to an environmental variable, but invariably, information might be lost or become biased in the process of noise reduction. A common saying, sometimes attributed to the mathematician Edward W. Ng, goes “one man’s noise is another man’s signal”. Two types of noise can be distinguished in tree-ring studies. First, as described by the principle of aggregated tree growth [3,7], tree-ring properties are the product of multiple factors. Investigating only one of these factors without accounting for the others means every other factor contributes to the ‘noise’. For example, the effect of nitrogen deposition is seen as noise when a drought signal is investigated, even though it has been shown that nitrogen deposition alters drought sensitivity [32]. Second, sensitivity to the same environmental factor can differ between individuals or different time periods [33–35]. Micro-site differences or competition not only have a direct effect on tree growth, but also indirectly modulate growth by altering the sensitivity of trees to other factors [6,19,20,32,36]. We therefore argue for utilization of the ‘noise’ and the exploration of individual growth differences.

1.3. Individual Based Assessments

The arguments above indicate that individual-based assessments of tree growth can potentially reveal additional insights into forest and treeline growth. For example, when climate correlations are explored, the frequency distribution of correlation coefficients can show if a few trees show a strong response or many trees show a medium response. Investigating the spatial distributions of trees with higher and lower correlation coefficients could identify site heterogeneities. Recently, temporally unstable climate correlations, termed the ‘divergence problem’, have been reported more frequently [35–37]. Of course, it would be of interest if this temporal phenomenon was distributed spatially (e.g., along temperature or moisture gradients). For example, at treeline sites the individual response to the divergence phenomenon might differ along the forest–tundra gradient [38]. Tree-level metadata, such as information on the spatial position of trees within a plot, tree height, crown-base height, crown diameter, social status, vitality, age, or competition indices, enhances individual-based analyses and can often easily be recorded directly in the field. Even though it requires considerable work and additional expertise, genetic analyses can provide data that can be used to identify clones [39], or a link between tree-ring traits and specific genes [40]. However, the genetic effect on growth within a site is likely low compared to the environmental variables [41].

The purpose of this study is to demonstrate, using an exemplary white spruce (*Picea glauca* (Moench) Voss) dataset, that individual-based assessments can offer additional insights into tree growth and ecosystem dynamics. We outline four simple but effective individual-based methods for the visual assessment of tree-ring datasets that describe tree and forest growth, as well as their environment control, in more detail than mean population chronologies can provide.

2. Materials and Methods

2.1. Site, Sampling and Data

To assess the possibilities of various individual tree assessment-methods, we used data from a white spruce (*Picea glauca* (MOENCH) Voss) treeline site at a steep (12–34°) south exposed bluff near Fairbanks, Alaska (64.70° N, 148.31° W). We hypothesized that the steep angle of incidence causes higher evapotranspiration, and consequently, water limited tree growth. A 1 ha plot was established in 2015 where all trees ($N = 327$) with a diameter at breast height (DBH) > 5 cm were sampled by extracting two cores per tree, or one core for small trees (DBH < 10 cm), to reduce damage to the tree. Cores were then mounted on wooden lathes and the surface was prepared with a core microtome [42]. Ring widths were measured from optical scans (Epson Perfection V700 Photo flatbed scanner, Nagano, Japan, 3200 dpi) with CooRecorder and were cross-dated visually with CDendro 8.1 (Cybis Elektronik

& Data AB, Saltsjöbaden, Sweden) [43]. Measurements of cores from the same tree were averaged. In addition, metadata for each tree was recorded in the field, including, tree height, DBH, crown diameter, crown base height, vitality (1 = best to 5 = dead), social status (open grown, dominant, codominant, intermediate, and suppressed), and spatial position (S100, SunNav Technology Co., Ltd., Tianjin, China, Differential Global Navigation System). The tree coordinates and DBH were used to calculate a neighborhood competition index (NCI, [44]) for each tree.

Monthly climate data (precipitation sum, mean temperature, mean potential evapotranspiration (PET), and vapor pressure) were downloaded from the Scenarios Network for Alaska and Arctic Planning (SNAP) for the period 1901–2009 [45], and the standardized precipitation evapotranspiration index (SPEI, [46]) was calculated from this data with the R package SPEI [47] for 6 (SPEI6) and 9 (SPEI9) months. Because we only intended to investigate climate sensitivity and not reconstruct climate or model tree growth, we detrended both tree-ring and climate data with a 30-year cubic smoothing spline using the *dplR* package [48] in R 3.2.3 [49]. The resulting tree-ring indices (TRI) and climate indices preserve the high-frequency signal (year–year variability) for the assessment of climate–growth correlations, and reduce spurious correlations due to non- or weakly-connected long-term trends in radial growth and climate. Autocorrelation was removed from the tree-ring series (prewhitening) by utilizing the *detrend* function with the *Ar* method within *dplR*.

2.2. Climate Correlations

Whole period and moving window climate correlations were computed for all individual tree chronologies. Correlations were computed with the six climate variables for all months of the previous year and January–September of the current year (21 months), resulting in $6 \times 21 = 126$ correlation values per tree. Running the same correlations with a moving window (20 years width, one year offset) over the period where climate data was available (109 years) resulted in up to $6 \times 21 \times (109 - 30) = 9954$ correlations per tree; though less for trees younger than the climate records. Given several hundred trees per site, this huge number illustrates why calculating arithmetic means as an intermediate step is warranted to make the results interpretable. With the methods described below, we attempt to supplement such averaging with individual analyses.

2.3. Jitterplots of Climate Correlations

Monthly climate correlations are often illustrated with the month on the x -axis and the correlation coefficients on the y -axis, sometimes including confidence intervals. Analogue to such figures, for example, are those produced by the *dcc* function in the R package *treeclim* [50]; jitter plots can be used to show the correlation values of all individual trees [24]. In addition to showing how frequent certain correlation values are, jitter plots also facilitate using metadata, such as age or competition index, as color. This allows the identification of trees that are more (or less) sensitive to a climate variable. The *geom_jitter* function in the R-package *ggplot2* [51] is one way to implement this concept in R.

2.4. Individual Tree Moving Window Correlations

Temporally unstable climate correlations, sometimes called the divergence problem [37], have been reported by various studies and its causes are still unclear [34,37,52]. Divergent growth can be assessed using methods such as moving window correlations (described above). While normal histograms show the frequency distribution of correlation values in one period, heat maps with a color scale for these frequencies are required to demonstrate how these frequency distributions change over time. The advantage of using moving window correlations with a single mean population chronology is that temporal changes in the variance of correlation values among individuals can become evident.

2.5. Spatial Distribution Maps

Recording tree coordinates within a plot is advantageous because it facilitates assessment of the spatial distribution of individual-tree climate sensitivity. Most sites can be assumed to have some microsite differences, even though they might not be obvious in the field. Microsite variability is caused by multiple factors, including, soil depth differences, above- or below- ground water runoff, organic matter accumulation in depressions, distribution of other competitive or symbiotic organisms, the effect of shading on photosynthetically active radiation, temperature, and evapotranspiration. Environmental gradients, such as the treeline datasets used in this study, are also particularly suitable for spatial analyses, because they cover environmental gradients. Furthermore, the incorporation of moving window climate correlations adds a time component to examine temporal variability in spatial patterns of climate sensitivity. In print, multiple maps are required to visualize spatio-temporal dynamics properly, however, in digital media, plots of multiple time windows can be combined into a video or animation.

2.6. The t-SNE Method to Assess Tree Similarities

Most scientific plots only use two dimensions (x and y axis), as more than four dimensions, after adding a z -axis and colors, are almost impossible to display within one plot. However, many datasets that describe more than four properties of any individual or item would require more dimensions to be plotted. For example, the ring width of one year can be interpreted as one trait and would require one dimension per year if not plotted as a time series. Similarly, climate growth correlations for multiple climate variables would require more dimensions to be plotted (e.g., 126 dimensions/climate variables in this study). Many correlations are appropriate because tree growth is a process that takes place over the whole vegetation period; winter months also affect growth via snow fall, snow melt water, and extreme events, and even the months of previous years can affect reserves (non-structural carbohydrates, NSCs), buds formed for the next year, or needles persisting multiple years, in the case of evergreen conifers. Thus, it can be desirable to identify trees with similar tree ring patterns or similar climate responses to identify what makes trees more similar or different. Clustering methods are an approach to assess similarity. Common clustering methods, like the k -means algorithm [53], require users to predefine a (more or less meaningful) discrete number of clusters. Principal component analyses (PCA), on the other hand, assesses commonality between variables, which is often employed just to visualize the first two principal components in biplots, resulting in the loss of individual information. However, developments like the principal component gradient analysis [31] show the utility of such methods and validate the interest of the tree-ring community in intra-site differences in climate sensitivity.

t -distributed Stochastic Neighbor Embedding (t -SNE [54]), which originated from machine learning algorithms to reduce multi-dimensional data and create 2D plots, could be a more suitable method to assess why certain trees have similar climate responses. Points corresponding to trees with more similar tree-ring patterns or climate responses are plotted closer to each other. Thus, trees are not assigned to discrete clusters, but the distance between two points/trees in a t -SNE plot reflects their similarity on a continuous scale. We created t -SNE plots with the R-package *Rtsne* [55] using the TRI data and the 126 climate correlations for each tree. t -SNE plots based on TRI will highlight which trees have similar year–year variability in tree-ring width (high-frequency signal). Analogous to TRI, t -SNE plots based on the climate correlations of each tree will illustrate which trees have similar climate sensitivity. As with PCAs, the t -SNE method cannot handle missing values, therefore, a tradeoff decision between including younger trees and including tree-ring data over a longer time period had to be made. We chose to exclude the youngest 10% of the trees in the TRI t -SNE analysis, and we only used the climate-growth correlations of the last moving windows (1980–2009) for the respective climate sensitivity t -SNE analysis.

3. Results

3.1. Jitterplots

The correlations between climate and individual trees varied significantly for most climate variables, but often ranged between -0.5 and $+0.5$ (Figure 1A). Detrending procedures (30-year cubic smoothing spline and prewhitening) reduced this variance significantly (Figure 1A,B). Correlation coefficients of the mean population chronology mostly indicated stronger correlations than would be expected by the mean individual tree coefficients. Indicated by the color gradients in Figure 1, differences between the sensitivity of individual trees to April SPEI9 appeared to be related to competition (NCI). We observed that the detrending of the tree-ring width and climate data switched which trees were most sensitive to April SPEI9, and in many cases even switched the sign of the correlation (Figure 1A,B). After detrending, trees with a lower NCI, i.e., trees closer to the treeline edge with fewer neighbors, were most sensitive. The effect of detrending on the climate–growth correlations is discussed in Supplementary Material Figure S1.

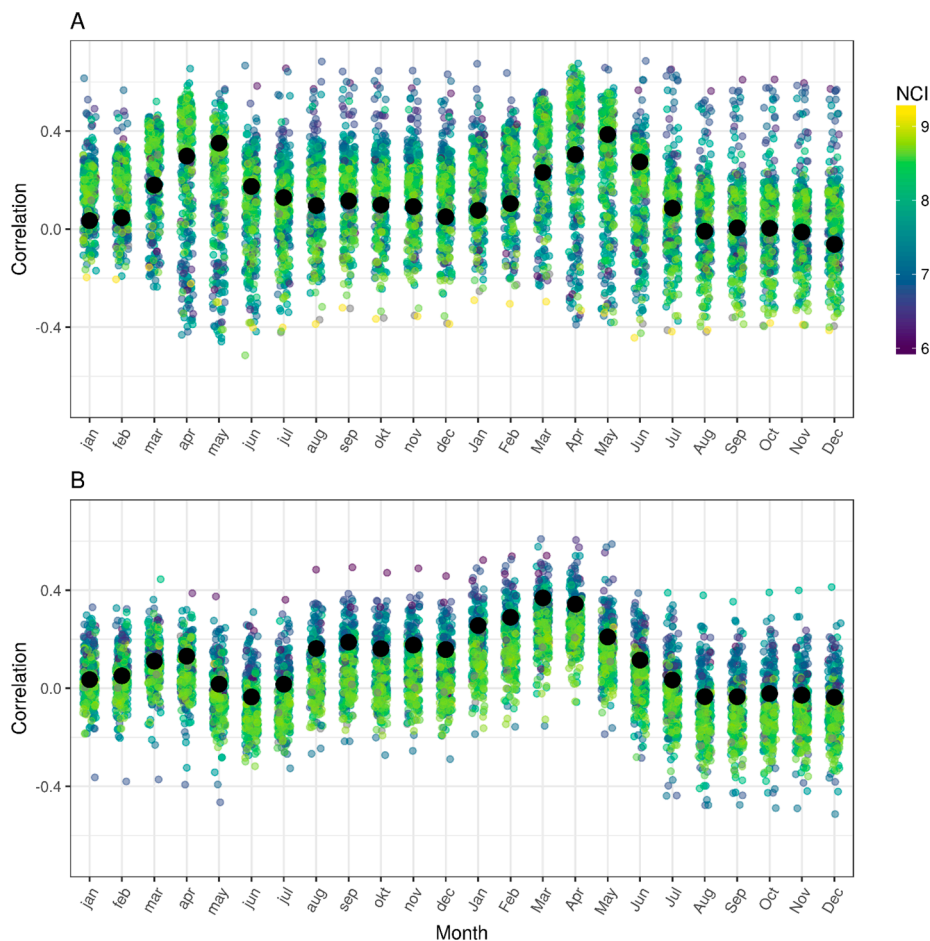


Figure 1. Jitterplot of (A) Pearson correlation coefficients of the raw tree-ring width with the SPEI9 for individual trees (small colored points) and for the mean population chronology (big black points). The neighborhood competition index (NCI) was used as color scale for individual trees; (B) the same correlations as in (A), but using detrended ring width (tree-ring indices (TRI)) and SPEI9 time-series (30-year cubic smoothing spline and ring width was additionally prewhitened).

3.2. Individual Tree Moving Window Correlations

Heat maps were used to assess ‘individual tree moving window climate correlations’, and described the frequency distribution of correlation values in each time window (3D histograms). Figure 2 shows three examples of the general patterns that heatmaps can provide, in particular, stability over time, changes over time, and variance differences between climate variables. For example, climate correlations were comparatively strong and stable over time, showing no changes in mean, variance, and skewness of the distributions for April SPEI9 (Figure 2A). However, more frequently, these distribution parameters changed over time (e.g., June temperature, Figure 2B). Typically, these distributions were normally distributed at mean correlation values around zero, and became skewed toward zero at higher or lower mean values. The variance can also differ slightly between climate variables, as shown in Figure 2A,C, though much larger variances can be found at other sites (not shown).

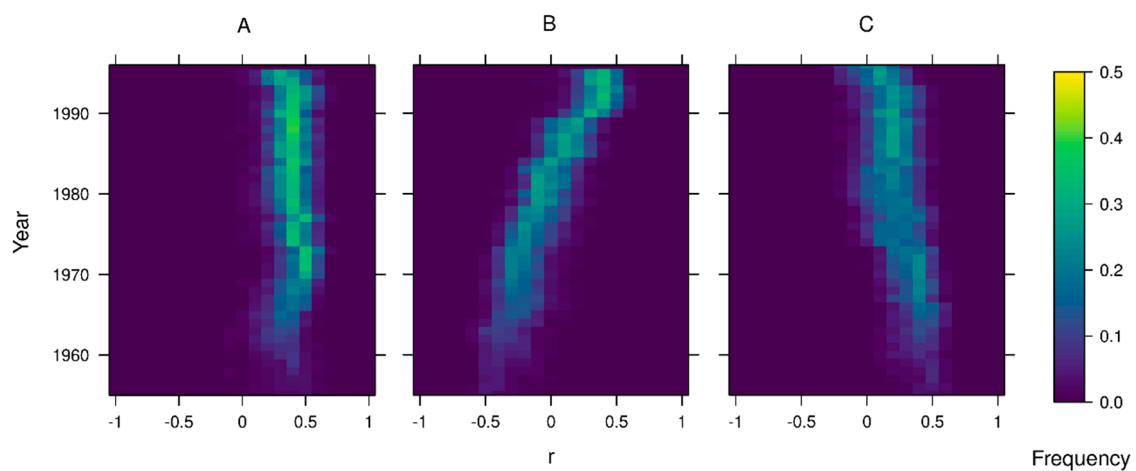


Figure 2. Frequency distributions (3D histograms) of individual tree correlation values with climate variables over time (30 year moving window). (A) correlation of individual TRI with April SPEI9; (B) correlations with June temperature; (C) correlations with previous year August SPEI6.

3.3. Spatial Distribution Maps

The climate sensitivity of individual trees displayed a random spatial distribution in the plots for most climate variables. However, in some cases spatio-temporal patterns emerged. By comparing Figure 3A,B, the initial absence of spatial patterns is visible in the period 1969–1988 when all trees showed a similar sensitivity to April SPEI9. Interestingly, between 1989–2008, further away from the treeline edge, and particularly for trees growing at more northerly locations, sensitivity to April SPEI9 declined (Figure 3). This corresponds to the drought gradient anticipated by the treeline formation. Spatio-temporal dynamics for April SPEI9 and all other climate variables are also visualized as videos in Supplementary Material Video S1.

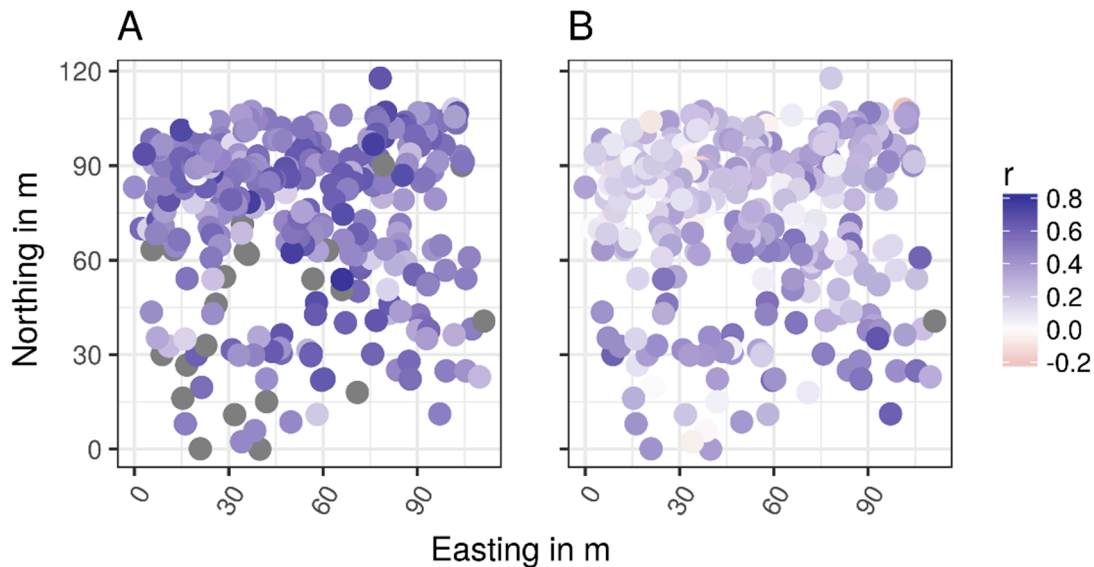


Figure 3. Spatial distribution of the correlation coefficients of individual TRI with April SPEI9. (A) shows the correlation for the period 1969–1988 and (B) for the period 1989–2008. Grey dots show trees for which no climate correlations could be calculated due to young age and thus insufficient data in the respective time period.

3.4. Similar Tree Ring Patterns and Climate Sensitivity

The t-SNE method visualizes trees which were more similar or more different regarding their TRI pattern and climate correlations, with more similar trees plotted closer to each other. Similarity between individual-tree ring-width patterns and climate-growth correlations of the 126 climate variables varied, but did not exhibit distinct groupings. However, superimposing the t-SNE plot with color scales based on tree metadata reveals the parameters that contribute to tree growth and climate sensitivity. The t-SNE plots show that trees with a similar TRI pattern or similar climate sensitivity also had a similar crowding index (Figure 4). However, there are some exceptions where several trees with a low NCI have a climate sensitivity more similar to that of trees with a high NCI.

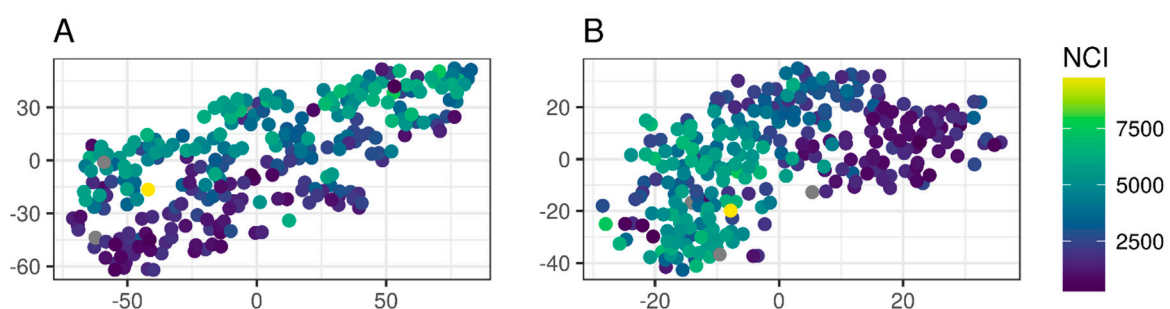


Figure 4. t-distributed Stochastic Neighbor Embedding (t-SNE) plots for (A) TRI patterns and (B) climate correlations with each point representing one tree. Points of more similar trees are plotted closer together and the neighborhood competition index (NCI) was used as color scale. Axes in t-SNE plots are dimensionless.

4. Discussion

The tree-ring patterns of individual trees differ at the site-level, which appears to be partly caused by differences in individual responses to climate variability. Depending on the target research question(s) and spatial scale of application, it can be useful to remove these differences by averaging

all individuals, or, as demonstrated here, various methods can explore these differences systematically and aid the ecological interpretation of the results. Our research highlights that tree metadata, like age, height, crowding indices, or microsite differences can be used to assess climatic growth-drivers in more detail.

4.1. Variances

The frequency distributions of climate correlations gradually highlighted that some climate variables correlated with all trees similarly and continuously throughout time, indicating that this climate parameter influences the growth of all trees at a site (e.g., April SPEI9, Figure 2A). In contrast, we also found that climate sensitivity can vary significantly over time (e.g., June temperature, Figure 2B [35–37]) or show a higher variance (e.g., previous year August SPEI6, Figure 2C). Highly variable climate sensitivity can be caused by differences in microsite conditions and individual-tree parameters like age, height, or competition [25,56,57]. Climate correlations with population chronologies do not consider these individual differences and provide only one correlation value. Thus, as with all averaging procedures, the underlying distribution of the data is lost. Our results indicate that skewness in the distribution of correlation values increases with the mean value. In this case, climate sensitivity may be underestimated by climate correlations with population chronologies. Interpreting population-level climate-correlations with respect to population statistics like the SSS [14,17] does not solve this problem either, because these measures are not directly linked to single environmental variables, but the overall variance between individuals. The variability in the climate sensitivity of individual trees generally calls for further analyses to determine potential causes.

4.2. Individual Metadata Effects on Climate Sensitivity

Variability in individual tree growth, as pointed out above, emphasizes the importance of collecting tree-level metadata. In this study, metadata that quantified individual differences provided valuable information on the causes of different climate sensitivities. The jitter plots (Figure 1) indicated the variables that could affect climate sensitivity, such as the neighborhood competition index NCI at our study site (Figure 1). On the downside, multicollinearity between metadata variables can complicate these investigations. In our case, trees with a higher crowding index were also taller, likely because vertical growth is promoted by competition for light [58,59].

The spatial distribution of the climate correlations of individual trees does indicate an environmental gradient at the site (Figure 3). In other studies, such maps might not just indicate gradients, but also local spots or groups of trees with different climate sensitivity. Furthermore, metadata was crucial for the t-SNE method. t-SNE plots, based on TRI and climate correlation values, did not show discrete clusters (i.e., a group of trees separated far from other trees). However, the distribution of trees in the t-SNE plots indicated that trees did differ regarding their TRI pattern and their climate sensitivity, with variability expressed continuously and not in discrete clusters. Superimposing metadata color-scales in the t-SNE plots revealed potential variables that could make trees more similar or different. As already indicated by the jitter plots, the crowding index appeared to affect climate sensitivity at our study site (Figure 4B). The t-SNE plots based on TRI are potentially useful in the absence of strong climate–growth relationships and can help identify what factors limit tree growth. Furthermore, t-SNE plots based on many climate correlations, as in Figure 4B, can be used to illustrate an individual-tree climate-sensitivity fingerprint. This can be used to identify trees that are generally more sensitive to drought related parameters due to their root system, wood anatomy, or microsite. Such trees will likely not just show a higher sensitivity to one monthly climate variable, but a whole set of moisture related variables.

Various potential mechanisms could explain why climate sensitivity varies along certain metadata gradients. For example, competition for resources, like water, could modulate climate sensitivity. In particular, asymmetric competition, meaning that the competitive power scales under or over-proportional to tree-size, could vary individual water availability [60–62]. As trees

grow taller with age, their wood anatomy changes (conduit tapering [56,57,63]), which increases hydraulic resistance, and thus, could also increase drought susceptibility [64,65]. In theory, genetic or epigenetic differences could also alter climate sensitivity, although, this has usually only been shown in provenance trials [40], not for natural within-site genetic variation [41].

4.3. Potential Further Analyses

Some of the differences in tree-level climate sensitivity can be explained, and should not necessarily be treated as noise. Earlier studies have shown that parameters like competition, nitrogen deposition, and tree-height-related wood anatomical changes affect climate sensitivity [19–21,32,59,66]. In this study, we demonstrated how to visually detect potential causes of different climate sensitivities. We suggest that more advanced statistical analyses and tree-growth models are needed to describe climate-growth relationships more realistically. As the principal of aggregated tree growth already indicates, there is an almost infinite number of variables that directly affect tree growth [2,3], which are often modulated by other variables. Additionally, ‘complete’ tree growth models would have to account for the various physiological processes within a tree, e.g., photosynthesis and cambial activity, and separate how each process affects tree-ring parameters. Such models are not yet possible, leaving scientists to use more basic methods, like climate correlations with mean chronologies. However, increasing sample sizes and newer statistical methods allow for analyses that include the individual variables visualized in our study.

One advantage of simply averaging multiple individual tree chronologies is that it avoids pseudoreplications in statistical analyses. However, methods exist that can account for pseudoreplications while not relying on the computation of mean values. Mixed models can accomplish this via random effects [5,67], and have successfully been applied to tree-ring datasets [30]. For example, tree IDs can be used as random intercepts in mixed models. These random intercepts, sometimes called the nuisance variable, can consider that some trees grow more or less without exactly knowing why. More complex mixed models might also incorporate random slopes [5], which could be used to account for individual climate-sensitivities. Generally, variable interactions can be used in various model types to account for modulations of climate sensitivity by additional variables like tree height or crowding indices. Lastly, process based and agent based models (ABM) are promising tools that have become increasingly popular. Process based models can be used to model the growth rate/process over the course of the year, though they can be difficult to fit [68,69]. Agent based models can be particularly suitable to account for interactions between individuals (agents), such as competition for light and water [70,71].

5. Conclusions

This article addresses the principle of aggregated tree growth and the accumulating evidence that various parameters influence the climate sensitivity of individual trees, such as, competition [21,25,66], age [29,57], and height [56,59]. The methods described here highlight individual tree differences and potential causes. In tree-ring science applications, inferring the general effects of climate on overall tree growth from single individuals is not possible [24], nor appropriate, thus, the principle of sample replication has become extremely important in tree-ring studies. However, tree metadata is becoming increasingly available, and as sample sizes increase, site-level may not be the best methodological option anymore. Thus, we agree with the assessment of Lloyd et al. [6], who argued for the integration of dendrochronology with other disciplines that can provide metadata. The methods described in this article are therefore intended to promote individual-based analyses of tree-ring datasets and the exploitation of tree metadata, with the ultimate goal of contributing to a better understanding of tree growth and its driving factors.

Supplementary Materials: The following are available online at <http://www.mdpi.com/1999-4907/9/4/216/s1>. Figure S1: (A) mean annual growth and the respective trend-line for trees with a lower and a higher neighborhood

competition index (NCI). (B) time-series of the April SPEI9 with its trend-line, Videos S2: Spatio-temporal dynamics of climate sensitivity shown for all climate variables.

Acknowledgments: This project was funded by the German Research Foundation (DFG) within the Research Training Group RESPONSE (DFG RTG 2010). We thank Glenn Juday, Ryan Jess, and Jamie Hollingsworth for supporting our work and their expertise. In addition, we would like to thank Jelena Lange, Renate Hefner, Franziska Eichhorn, Brook Anderson, and Tobias Scharnweber for their help during fieldwork.

Author Contributions: M.T., D.W., M.S. and M.W. conceived the plot setup and collected the samples with the help of others (see acknowledgements). M.T. analyzed the data with the help of M.W. and M.v.d.M.-T.; Methods and ecological implications were discussed by M.T., M.v.d.M.-T., J.E.H., D.W., M.S. and M.W.; M.T. drafted the original manuscript together with J.E.H., M.W. and M.v.d.M.-T.; all authors revised and refined the final manuscript.

Conflicts of Interest: The authors declare no conflicts of interest.

References

1. Cook, E.R.; Kairiukstis, L.A. *Methods of Dendrochronology: Applications in the Environmental Sciences*; Springer Science & Business Media: Dordrecht, The Netherlands, 2013; ISBN 978-94-015-7879-0.
2. Fritts, H.C. *Tree Rings and Climate*; The Blackburn Press: Caldwell, NJ, USA, 1976; ISBN 978-1-930665-39-2.
3. Speer, J.H. *Fundamentals of Tree-Ring Research*; University of Arizona Press: Tucson, AZ, USA, 2010.
4. Hurlbert, S.H. Pseudoreplication and the design of ecological field experiments. *Ecol. Monogr.* **1984**, *54*, 187–211. [[CrossRef](#)]
5. Zuur, A.F. *Mixed Effects Models and Extensions in Ecology with R*; Statistics for Biology and Health; Springer: New York, NY, USA, 2009.
6. Lloyd, A.H.; Sullivan, P.F.; Bunn, A.G. Integrating dendroecology with other disciplines improves understanding of upper and latitudinal treelines. In *Dendroecology*; Ecological Studies; Springer: Cham, Switzerland, 2017; pp. 135–157.
7. Cook, E.R. A Time Series Analysis Approach to Tree Ring Standardization. Ph.D. Thesis, University of Arizona, Tucson, AZ, USA, 1985.
8. Kelly, D. The evolutionary ecology of mast seeding. *Trends Ecol. Evol.* **1994**, *9*, 465–470. [[CrossRef](#)]
9. Martín-Benito, D.; Kint, V.; del Río, M.; Muys, B.; Cañellas, I. Growth responses of West-Mediterranean *Pinus nigra* to climate change are modulated by competition and productivity: Past trends and future perspectives. *For. Ecol. Manag.* **2011**, *262*, 1030–1040. [[CrossRef](#)]
10. Sullivan, P.F.; Pattison, R.R.; Brownlee, A.H.; Cahoon, S.M.P.; Hollingsworth, T.N. Limited evidence of declining growth among moisture-limited black and white spruce in interior Alaska. *Sci. Rep.* **2017**, *7*, 15344. [[CrossRef](#)] [[PubMed](#)]
11. Sherriff, R.L.; Miller, A.E.; Muth, K.; Schriver, M.; Batzel, R. Spruce growth responses to warming vary by ecoregion and ecosystem type near the forest-tundra boundary in south-west Alaska. *J. Biogeogr.* **2017**, *44*, 1457–1468. [[CrossRef](#)]
12. Schweingruber, F.H.; Kairiukstis, L.; Shiyatov, S. Sample Selection. In *Methods of Dendrochronology: Applications in the Environmental Sciences*; Cook, E.R., Kairiukstis, L.A., Eds.; Springer Science & Business Media: Dordrecht, The Netherlands, 1990.
13. Körner, C. *Alpine Treelines: Functional Ecology of the Global High Elevation Tree Limits*; Springer Science & Business Media: Basel, Switzerland; Heidelberg, Germany; New York, NY, USA; Dordrecht, The Netherlands; London, UK, 2012.
14. Wigley, T.M.L.; Briffa, K.R.; Jones, P.D. On the average value of correlated time series, with applications in dendroclimatology and hydrometeorology. *J. Clim. Appl. Meteorol.* **1984**, *23*, 201–213. [[CrossRef](#)]
15. Douglass, A. *Climate Cycles and Tree-growth*; Carnegie Institution of Washington: Washington, DC, USA, 1936.
16. Bunn, A.G.; Jansma, E.; Korpela, M.; Westfall, R.D.; Baldwin, J. Using simulations and data to evaluate mean sensitivity ($\bar{\zeta}$) as a useful statistic in dendrochronology. *Dendrochronologia* **2013**, *31*, 250–254. [[CrossRef](#)]
17. Buras, A. A comment on the expressed population signal. *Dendrochronologia* **2017**, *44*, 130–132. [[CrossRef](#)]
18. Trugman, A.T.; Medvigy, D.; Anderegg, W.R.L.; Pacala, S.W. Differential declines in Alaskan boreal forest vitality related to climate and competition. *Glob. Chang. Biol.* **2018**. [[CrossRef](#)] [[PubMed](#)]

19. Price, D.T.; Cooke, B.J.; Metsaranta, J.M.; Kurz, W.A. If forest dynamics in Canada's west are driven mainly by competition, why did they change? Half-century evidence says: Climate change. *Proc. Natl. Acad. Sci. USA* **2015**, *112*, E4340. [[CrossRef](#)] [[PubMed](#)]
20. Zhang, J.; Huang, S.; He, F. Half-century evidence from western Canada shows forest dynamics are primarily driven by competition followed by climate. *Proc. Natl. Acad. Sci. USA* **2015**, *112*, 4009–4014. [[CrossRef](#)] [[PubMed](#)]
21. Wang, Y.; Pederson, N.; Ellison, A.M.; Buckley, H.L.; Case, B.S.; Liang, E.; Julio Camarero, J. Increased stem density and competition may diminish the positive effects of warming at alpine treeline. *Ecology* **2016**, *97*, 1668–1679. [[CrossRef](#)] [[PubMed](#)]
22. Konter, O.; Krusic, P.J.; Trouet, V.; Esper, J. Meet Adonis, Europe's oldest dendrochronologically dated tree. *Dendrochronologia* **2017**, *42*, 12. [[CrossRef](#)]
23. Turney, C.S.M.; Palmer, J.; Maslin, M.A.; Hogg, A.; Fogwill, C.J.; Southon, J.; Fenwick, P.; Helle, G.; Wilmshurst, J.M.; McGlone, M.; et al. Global peak in atmospheric radiocarbon provides a potential definition for the onset of the anthropocene epoch in 1965. *Sci. Rep.* **2018**, *8*, 3293. [[CrossRef](#)] [[PubMed](#)]
24. Carrer, M. Individualistic and time-varying tree-ring growth to climate sensitivity. *PLoS ONE* **2011**, *6*, e22813. [[CrossRef](#)] [[PubMed](#)]
25. Gleason, K.E.; Bradford, J.B.; Bottero, A.; D'Amato, A.W.; Fraver, S.; Palik, B.J.; Battaglia, M.A.; Iverson, L.; Kenefic, L.; Kern, C.C. Competition amplifies drought stress in forests across broad climatic and compositional gradients. *Ecosphere* **2017**, *8*. [[CrossRef](#)]
26. Choler, P.; Michalet, R.; Callaway, R.M. Facilitation and competition on gradients in alpine plant communities. *Ecology* **2001**, *82*, 3295–3308. [[CrossRef](#)]
27. Callaway, R.M.; Walker, L.R. Competition and facilitation: A synthetic approach to interactions in plant communities. *Ecology* **1997**, *78*, 1958–1965. [[CrossRef](#)]
28. Rohner, B.; Waldner, P.; Lischke, H.; Ferretti, M.; Thürig, E. Predicting individual-tree growth of central European tree species as a function of site, stand, management, nutrient, and climate effects. *Eur. J. For. Res.* **2017**, 1–16. [[CrossRef](#)]
29. Konter, O.; Büntgen, U.; Carrer, M.; Timonen, M.; Esper, J. Climate signal age effects in boreal tree-rings: Lessons to be learned for paleoclimatic reconstructions. *Quat. Sci. Rev.* **2016**, *142*, 164–172. [[CrossRef](#)]
30. Galván, J.D.; Camarero, J.J.; Gutiérrez, E. Seeing the trees for the forest: Drivers of individual growth responses to climate in *Pinus uncinata* mountain forests. *J. Ecol.* **2014**, *102*, 1244–1257. [[CrossRef](#)]
31. Buras, A.; van der Maaten-Theunissen, M.; van der Maaten, E.; Ahlgrimm, S.; Hermann, P.; Simard, S.; Heinrich, I.; Helle, G.; Unterseher, M.; et al. Tuning the voices of a choir: Detecting ecological gradients in time-series populations. *PLoS ONE* **2016**, *11*, e0158346. [[CrossRef](#)] [[PubMed](#)]
32. Ibáñez, I.; Zak, D.R.; Burton, A.J.; Pregitzer, K.S. Anthropogenic nitrogen deposition ameliorates the decline in tree growth caused by a drier climate. *Ecology* **2018**, *99*, 411–420. [[CrossRef](#)] [[PubMed](#)]
33. Driscoll, W.W.; Wiles, G.C.; D'Arrigo, R.D.; Wilmking, M. Divergent tree growth response to recent climatic warming, Lake Clark National Park and Preserve, Alaska. *Geophys. Res. Lett.* **2005**, *32*, L20703. [[CrossRef](#)]
34. Zhang, Y.; Wilmking, M. Divergent growth responses and increasing temperature limitation of Qinghai spruce growth along an elevation gradient at the northeast Tibet Plateau. *For. Ecol. Manag.* **2010**, *260*, 1076–1082. [[CrossRef](#)]
35. Wilmking, M.; D'Arrigo, R.; Jacoby, G.C.; Juday, G.P. Increased temperature sensitivity and divergent growth trends in circumpolar boreal forests. *Geophys. Res. Lett.* **2005**, *32*, L15715. [[CrossRef](#)]
36. Ponocná, T.; Chuman, T.; Rydval, M.; Urban, G.; Migała, K.; Tremel, V. Deviations of treeline Norway spruce radial growth from summer temperatures in East-Central Europe. *Agric. For. Meteorol.* **2018**, 253–254, 62–70. [[CrossRef](#)]
37. D'Arrigo, R.; Wilson, R.; Liepert, B.; Cherubini, P. On the 'Divergence Problem' in Northern Forests: A review of the tree-ring evidence and possible causes. *Glob. Planet. Chang.* **2008**, *60*, 289–305. [[CrossRef](#)]
38. Wilmking, M.; Juday, G.P. Longitudinal variation of radial growth at Alaska's northern treeline—recent changes and possible scenarios for the 21st century. *Glob. Planet. Chang.* **2005**, *47*, 282–300. [[CrossRef](#)]
39. Wilmking, M.; Buras, A.; Eusemann, P.; Schnittler, M.; Trouillier, M.; Würth, D.; Lange, J.; van der Maaten-Theunissen, M.; Juday, G.P. High frequency growth variability of White spruce clones does not differ from non-clonal trees at Alaskan treelines. *Dendrochronologia* **2017**, *44*, 187–192. [[CrossRef](#)]

40. Housset, J.M.; Nadeau, S.; Isabel, N.; Depardieu, C.; Duchesne, I.; Lenz, P.; Girardin, M.P. Tree rings provide a new class of phenotypes for genetic associations that foster insights into adaptation of conifers to climate change. *New Phytol.* **2018**. [[CrossRef](#)] [[PubMed](#)]
41. King, G.M.; Gugerli, F.; Fonti, P.; Frank, D.C. Tree growth response along an elevational gradient: Climate or genetics? *Oecologia* **2013**, *173*, 1587–1600. [[CrossRef](#)] [[PubMed](#)]
42. Gärtner, H.; Nievergelt, D. The core-microtome: A new tool for surface preparation on cores and time series analysis of varying cell parameters. *Dendrochronologia* **2010**, *28*, 85–92. [[CrossRef](#)]
43. Cybis Elektronik & Data AB. In Coorecorder; Saltsjöbaden, Sweden. Available online: <http://www.cybis.se/indexe.htm> (accessed on 19 April 2018).
44. Canham, C.D.; LePage, P.T.; Coates, K.D. A neighborhood analysis of canopy tree competition: Effects of shading versus crowding. *Can. J. For. Res.* **2004**, *34*, 778–787. [[CrossRef](#)]
45. SNAP Scenarios Network for Alaska and Arctic Planning 2016; University of Alaska, Fairbanks, USA. Available online: <http://ckan.snap.uaf.edu/dataset> (accessed on 19 April 2018).
46. Vicente-Serrano, S.M.; Beguería, S.; López-Moreno, J.I. A multiscale drought index sensitive to global warming: The standardized precipitation evapotranspiration index. *J. Clim.* **2009**, *23*, 1696–1718. [[CrossRef](#)]
47. Beguería, S.; Vicente-Serrano, S.M. SPEI: Calculation of the Standardised Precipitation-Evapotranspiration Index; R Package Version 1.6. 2013. Available online: <https://CRAN.R-project.org/package=SPEI> (accessed on 19 April 2018).
48. Bunn, A.G. A dendrochronology program library in R (dplR). *Dendrochronologia* **2008**, *26*, 115–124. [[CrossRef](#)]
49. R Core Team. *R: A Language and Environment for Statistical Computing*; R Foundation for Statistical Computing: Vienna, Austria, 2015.
50. Zang, C.; Biondi, F. treeclim: An R package for the numerical calibration of proxy-climate relationships. *Ecography* **2015**, *38*, 431–436. [[CrossRef](#)]
51. Wickham, H. *ggplot2: Elegant Graphics for Data Analysis*; Springer: New York, NY, USA, 2009.
52. Wilmking, M.; Scharnweber, T.; van der Maaten-Theunissen, M.; van der Maaten, E. Reconciling the community with a concept—The uniformitarian principle in the dendro-sciences. *Dendrochronologia* **2017**, *44*, 211–214. [[CrossRef](#)]
53. Lloyd, S. Least squares quantization in PCM. *IEEE Trans. Inf. Theory* **1982**, *28*, 129–137. [[CrossRef](#)]
54. Van der Maaten, L.; Hinton, G. Visualizing Data using t-SNE. *J. Mach. Learn. Res.* **2008**, *9*, 2579–2605.
55. Krijthe, J.H. Rtsne: T-Distributed Stochastic Neighbor Embedding Using Barnes-Hut Implementation. 2015. Available online: <https://github.com/jkrijthe/Rtsne> (accessed on 19 April 2018).
56. Mencuccini, M.; Hölttä, T.; Petit, G.; Magnani, F. Sanio’s laws revisited. Size-dependent changes in the xylem architecture of trees. *Ecol. Lett.* **2007**, *10*, 1084–1093. [[CrossRef](#)] [[PubMed](#)]
57. Carrer, M.; Urbinati, C. Age-dependent tree-ring growth responses to climate in *Larix Decidua* and *Pinus Cembra*. *Ecology* **2004**, *85*, 730–740. [[CrossRef](#)]
58. King, D.A. The Adaptive Significance of Tree Height. *Am. Nat.* **1990**, *135*, 809–828. [[CrossRef](#)]
59. Koch, G.W.; Sillett, S.C.; Jennings, G.M.; Davis, S.D. The limits to tree height. *Nature* **2004**, *428*, 851–854. [[CrossRef](#)] [[PubMed](#)]
60. Weiner, J. Asymmetric competition in plant populations. *Trends Ecol. Evol.* **1990**, *5*, 360–364. [[CrossRef](#)]
61. Pretzsch, H.; Biber, P. Size-symmetric versus size-asymmetric competition and growth partitioning among trees in forest stands along an ecological gradient in central Europe. *Can. J. For. Res.* **2010**, *40*, 370–384. [[CrossRef](#)]
62. Linares, J.-C.; Delgado-Huertas, A.; Camarero, J.J.; Merino, J.; Carreira, J.A. Competition and drought limit the response of water-use efficiency to rising atmospheric carbon dioxide in the Mediterranean fir *Abies pinsapo*. *Oecologia* **2009**, *161*, 611–624. [[CrossRef](#)] [[PubMed](#)]
63. Sanio, K. *Über die Grosse der Holzzellen bei der Gemeinen Kiefer (Pinus silvestris)*; Leipzig publisher: Leipzig, Saxony, Germany, 1872; pp. 401–420.
64. Ryan, M.G.; Yoder, B.J. Hydraulic limits to tree height and tree growth. *BioScience* **1997**, *47*, 235–242. [[CrossRef](#)]
65. Ryan Michael, G.; Phillips, N.; Bond Barbara, J. The hydraulic limitation hypothesis revisited. *Plant Cell Environ.* **2006**, *29*, 367–381. [[CrossRef](#)]

66. Alam, S.A.; Huang, J.-G.; Stadt, K.J.; Comeau, P.G.; Dawson, A.; Gea-Izquierdo, G.; Aakala, T.; Hölttä, T.; Vesala, T.; Mäkelä, A.; Berninger, F. Effects of competition, drought stress and photosynthetic productivity on the radial growth of White Spruce in Western Canada. *Front. Plant Sci.* **2017**, *8*. [[CrossRef](#)] [[PubMed](#)]
67. Bates, D.; Mächler, M.; Bolker, B.; Walker, S. Fitting linear mixed-effects models using lme4. *arXiv* **2014**, *67*, 1. [[CrossRef](#)]
68. Vaganov, E.A.; Hughes, M.K.; Shashkin, A.V. *Growth Dynamics of Conifer Tree Rings: Images of Past and Future Environments*; Springer Science & Business Media: Dordrecht, The Netherlands, 2006.
69. Vaganov, E.A.; Anchukaitis, K.J.; Evans, M.N. How Well Understood Are the Processes that Create Dendroclimatic Records? A Mechanistic Model of the Climatic Control on Conifer Tree-Ring Growth Dynamics. In *Dendroclimatology; Developments in Paleoenvironmental Research*; Springer: Dordrecht, The Netherlands, 2011; pp. 37–75.
70. Pretzsch, H.; Biber, P.; Ďurský, J.; von Gadow, K.; Hasenauer, H.; Kändler, G.; Kenk, G.; Kublin, E.; Nagel, J.; Pukkala, T.; et al. Recommendations for standardized documentation and further development of forest growth simulators. *Forstw. Cbl.* **2002**, *121*, 138–151. [[CrossRef](#)]
71. Grimm, V.; Railsback, S.F. *Individual-Based Modeling and Ecology*; Princeton University Press: Princeton, NJ, USA, 2013.



© 2018 by the authors. Licensee MDPI, Basel, Switzerland. This article is an open access article distributed under the terms and conditions of the Creative Commons Attribution (CC BY) license (<http://creativecommons.org/licenses/by/4.0/>).